Separation Science and Technology
Publication details, including instructions for authors and subscription information:
http://www.informaworld.com/smpp/title~content=t713708471

Removal of Refractory Organics from Water by Aeration. II. Solvent Sublation of Methylene Blue and Methyl Orange

Joseph L. Womack[a]; Joel C. Lichter[a]; David J. Wilson[a]
[a] DepartmentS OF CHEMISTRY AND OF CIVIL AND ENVIRONMENTAL ENGINEERING, VANDERBILT UNIVERSITY NASHVILLE, TENNESSEE

To cite this Article Womack, Joseph L. , Lichter, Joel C. and Wilson, David J.(1982) 'Removal of Refractory Organics from Water by Aeration. II. Solvent Sublation of Methylene Blue and Methyl Orange', Separation Science and Technology, 17: 7, 897 — 924
To link to this Article: DOI: 10.1080/01496398208082102
URL: http://dx.doi.org/10.1080/01496398208082102

SEPARATION SCIENCE AND TECHNOLOGY, 17(7), pp. 897–924, 1982

Removal of Refractory Organics from Water by Aeration. II. Solvent Sublation of Methylene Blue and Methyl Orange

JOSEPH L. WOMACK, JOEL C. LICHTER, and DAVID J. WILSON*

DEPARTMENTS OF CHEMISTRY AND OF CIVIL AND ENVIRONMENTAL ENGINEERING
VANDERBILT UNIVERSITY
NASHVILLE, TENNESSEE 37235

Abstract

The solvent sublations of methylene blue–sodium tetradecylsulfate and of methyl orange–hexadecyltrimethylammonium bromide were carried out in lab-scale batch apparatus. Removal was from water to 2-octanol. Three possible mechanisms were examined in detail; the colored species removed in both cases is believed to consist of one ion of dye complexed with two of surfactant. Mass transfer rate effects in the vicinity of the bubble–water interface were examined theoretically, and the empirical time constant for mass transfer related to the lowest eigenvalue of a suitably selected diffusion problem.

*To whom correspondence should be addressed.

INTRODUCTION

In recent years there has been a great deal of interest in trace, potentially toxic, organic compounds in drinking water; this background is reviewed in our first paper of this series (*1*). It also has motivated our efforts toward the development of new, cheap, efficient methods to remove various types of organic compounds from aqueous systems. Our previous paper gave experimental data on the removal of methyl chloroform (1,1,1-trichloroethane) from water by aeration, and provided a mathematical model for this process which included mass transfer at the bubble–water interface as an important rate-limiting step.

Another aeration technique for the removal of some solutes from aqueous

systems is that of solvent sublation, first used by Sebba (*2*). In this procedure a surface-active solute is transported from the aqueous phase to an overlying layer of a nonvolatile organic liquid on the air–water interfaces of bubbles rising through the solvent sublation cell. Karger has written a review on the subject (*3*), and we included material on the subject in a more general review (*4*).

Sebba developed solvent sublation separations mainly for inorganic ions; he also noted that ionizable dyes could be selectively separated by adjustment of conditions and the use of suitable surface active agents. Caragay, Karger, and Lee separated methyl orange from rhodamine B with a cationic surfactant at a pH at which the methyl orange was anionic while the rhodamine B was zwitterionic (*5*, *6*). Karger, Pinfold, and Palmer carried out a detailed study of the solvent sublation of methyl orange–hexadecyltrimethylammonium ion pairs (*7*). These workers noted that solvent sublation can yield more complete separations than one would expect on the basis of equilibration of the solute between the aqueous and organic phases. They noted that the removal rate slowed down markedly as the separation proceeded—first-order kinetics were not obeyed—and they ascribed this to the gradually increasing concentration of the organic solvent (2-octanol) in the water layer. Sheiham and Pinfold investigated the solvent sublation of hexadecyltrimethylammonium chloride (*8*).

A number of metals have been separated from aqueous solution by solvent sublation. Bittner and his co-workers reported on Co(II), Fe(III), Ni(II), Pa(V), Th(IV), and U(VI) (*9*). Elhanan and Karger studied the sublation of $FeCl_4^-$ (*10*), and Spargo and Pinfold studied $Fe(CN)_6^{4-}$ (*11*). Szeglowski et al. have performed solvent sublation removals of europium, thulium, and ytterbium (*12*) and of americium and curium (*13*). More recently, Kotsuji and co-workers used a solvent sublation separation in the spectrophotometric determination of Fe(II) (*14*).

Other work in this area includes Stachurski and Szeglowski's theoretical treatment of solvent sublation as a random Markov process (*15*, *16*), and a study of phenol removal by solvent extraction, solvent sublation, and foam fractionation by Grieves et al. (*17*).

We present here experimental work on the solvent sublation of two dye–surfactant ion complexes, methylene blue–tetradecyl sulfate and methyl orange–hexadecyltrimethylammonium. 2-Octanol was used as the organic solvent. A lab-scale batch type apparatus of the sort previously described was used (*18*). The effects of varying air flow rate, ratio of reagents, and added salts were determined. We then examine three models for calculating removal rates: one which assumes that ion complex formation is complete and that the adsorption of ion pairs is governed by a Langmuir isotherm, and two in which mobile equilibria govern dye–surfactant complex formation and the adsorption isotherms of surfactant complexes are linear. We also

examine the factors affecting the rate of solute mass transfer to the rising bubble. The models are then compared with the experimental results.

EXPERIMENTAL

Fisher laboratory grade methylene blue (MeBlCl) was used to make a stock solution of 0.2985 g in 1.00 L of distilled water. Eastman reagent-grade sodium tetradecyl sulfate (NaTDS) was dissolved in distilled water to make a stock solution containing 0.0300 g of NaTDS per 100 mL of water. This solution was made fresh each week and kept refrigerated to inhibit bacterial decomposition. A methyl orange stock solution was made by dissolving 0.4974 g of Eastman practical-grade methyl orange in 1.00 L of distilled water. Eastman practical-grade hexadecyltrimethylammonium bromide (HTA) was prepared as a stock solution containing 0.4973 g/L of distilled water. Fisher certified grade $NaNO_3$, KCl, and NaH_2PO_4 were used to make 1.00% by weight stock solutions in distilled water. Appropriate quantities of the various stock solutions were then diluted to volume (usually 200 mL) with distilled water previously saturated with 2-octanol (Aldrich, technical).

The apparatus consisted of a 3.5 cm diam × 87 cm high Pyrex column fitted with a stopper at the bottom through which passed a "fine" fritted glass gas dispersion tube, a sampling stopcock, and a large clamped tube for fast drainage at the end of a run. House air was passed through a water saturator and glass wool filter before going to the gas dispersion tube. Air flow rates were measured on the filled column with a soap film flow meter and stopwatch. Air flow rates for the methylene blue runs ranged from 33.6 to 61.6 mL/min and averaged 56.6 mL/min. Air was run through the column continuously.

The usual 200 mL volume of test solution was made by pipetting the desired amount of methylene blue stock solution (usually 1.50 mL) into a 100-mL volumetric flask and diluting to 100 mL with octanol-saturated water. This solution was poured into another flask, and the 100 mL volumetric flask was then used to dilute the surfactant (usually 3.0 mL) plus any other materials (such as salts) to be added to the test solution. This was then diluted to 100 mL with octanol-saturated water and added to the diluted methylene blue solution. A 3-mL portion of the test solution was then used to prepare a standard calibration curve with a Beckman Model DB spectrophotometer. The volume of test solution was poured into the column, and immediately 1/10th that volume of 2-octanol was added and the timer started. Three-milliliter samples were taken for spectrophotometric analysis (645 nm) at 5 min intervals. Air flow measurements were made at 5 min intervals and averaged to obtain the air flow rate for the run.

The methyl orange–HTA runs differed only in that 0.75 mL methyl orange stock solution and 1.50 mL HTA stock solution were used to prepare the test solution, and 1 or 2 drops of 0.4 M HNO_3 were added to the samples to get greater sensitivity in the spectrophotometric analysis (495 nm).

Data were plotted as $\log_e [C_0/C(t)]$ versus t in minutes to clearly display any deviations from first-order kinetics, which would yield linear plots.

Eleven "standard" runs were made with 200 mL of test solution containing 1.40×10^{-6} mol of methylene blue and 2.85×10^{-6} mol of NaTDS. Figure 1 shows four of these runs. Air flow rates averaged 46.6 mL/min, and minor variations produced no observable changes in removal rate. First-order kinetics are obviously not being followed; the removal rate of methylene blue drops much too sharply after the first 10 min or so of the run. This was earlier noted by Karger et al. (*7*) with methyl orange–HTA; they ascribed it to the gradually increasing concentration of 2-octanol in the water layer. Since our water solutions were initially saturated with octanol and the octanol concentrations in our water layers could therefore decrease or remain constant but could not increase during the runs, this explanation appears to be inapplicable to our system, and should be reinvestigated in the system methyl orange–HTA. Exhaustive Soxhlet extraction of the surfactant with hexane caused no changes in the results.

The effects of three added salts were investigated in a set of 200 mL runs; Fig. 2 shows the results of adding various quantities of $NaNO_3$. There is a definite inhibiting effect observed at an $NaNO_3$ concentration of 3.7×10^{-3} M, and the rate of removal at a salt concentration of 5.9×10^{-2} M is roughly only one-fifth the rate of removal in the absence of added $NaNO_3$. Figure 3 displays runs inhibited with KCl, for which the effect is possibly somewhat greater than for $NaNO_3$, since 2.1×10^{-3} M KCl shows almost the same effect as 3.7×10^{-3} M $NaNO_3$. Figure 4 compares the effects of 0.0156% by weight of KCl, NaH_2PO_4, and $NaNO_3$, together with some more dilute NaH_2PO_4 solutions. KCl shows the greatest inhibition, probably because of its higher molar concentration, with perhaps a contribution from chloride complex formation with the methylene blue cation, as suggested by comparison with the $NaNO_3$ run. The NaH_2PO_4 run also appears to show a little more inhibition than would be expected from the $NaNO_3$ run, again suggesting the possibility of complex formation. These differences are not large, however. The top two plots show NaH_2PO_4 runs with molar ratios of salt to dye of about 1 to 1 for the top curve and 5 to 1 for the second highest. The 1 to 1 plot shows no significant deviation from that for a salt-free run.

Varying the surfactant concentration produces a large effect, as seen in Fig. 5. These were all 200 mL runs with methylene blue concentrations of 7.0×10^{-6} M and NaTDS to methylene blue molar ratios varying from 4

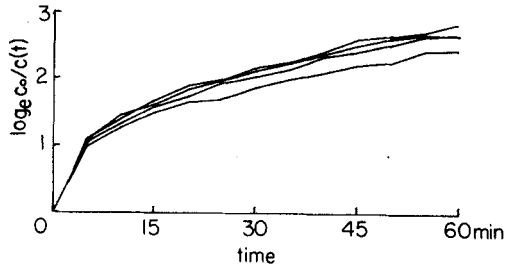

FIG. 1. Methylene blue–TDS standard runs; reproducibility of results. Concentrations were 7.0×10^{-6} *M* MeBl and 1.4×10^{-5} *M* NaTDS; average air flow rate was 56.6 mL/min.

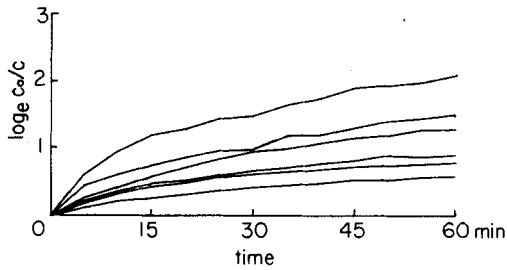

FIG. 2. Methylene blue–TDS; effect of added $NaNO_3$. Concentrations: MeBl, 7.0×10^{-6}; NaTDS, 1.4×10^{-5}; $NaNO_3$, 1.8, 3.7, 7.5, 15, 29, and 59×10^{-3} *M* from top to bottom.

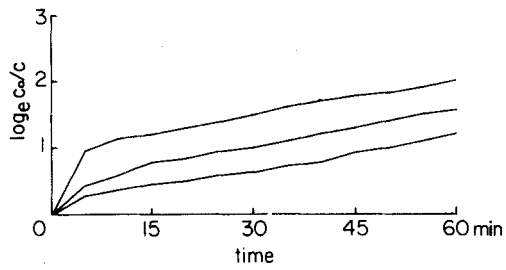

FIG. 3. Methylene blue–TDS; effect of added KCl. Concentrations: MeBl, 7.0×10^{-6}; NATDS, 1.4×10^{-5}; KCl, 1.05, 2.1, and 4.2×10^{-3} *M* from top to bottom.

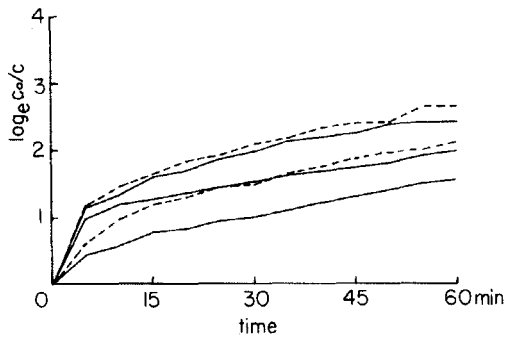

FIG. 4. Methylene blue–TDS; effects of different salts. MeBl and NaTDS concentrations are 7.0×10^{-6} and 1.4×10^{-5} M, respectively. The top run contains 7.5×10^{-6} M NaH_2PO_4; the second, 3.75×10^{-5} M NaH_2PO_4; the third, 1.8×10^{-3} M $NaNO_3$; the fourth, 1.1×10^{-3} M NaH_2PO_4; the bottom, 2.1×10^{-3} M KCl. The bottom three runs all contain 1/64% by weight added salt. The top run is indistinguishable from runs made without added salt.

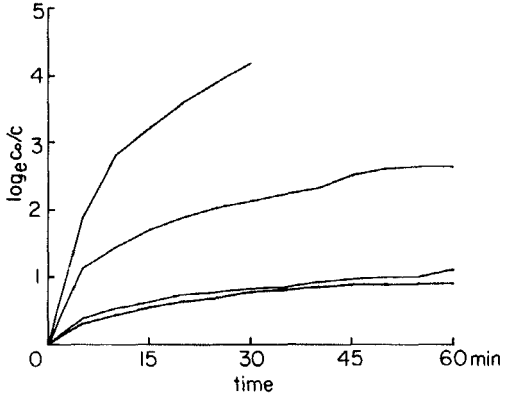

FIG. 5.Methylene blue–TDS; effect of NaTDS concentration. The MeBl concentration in all runs is 7.0×10^{-6} M; NaTDS concentrations from top to bottom are 28, 14, 4.7, and 3.5×10^{-6} M.

(the top run) to 0.5 (the bottom run). These results, the effects of added salts, and the curvature of the plots suggest that we are dealing with some sort of a mobile equilibrium between dye, surfactant, and complex.

The effect of increasing the volume of solution being treated is shown in Fig. 6; here the octanol:water volume ratio, air flow rate, and reagent concentrations were kept constant. We see the expected decrease in the rate of change of concentration. The dye–surfactant complex is extemely soluble in 2-octanol. One "standard" run was made without adding a layer of 2-

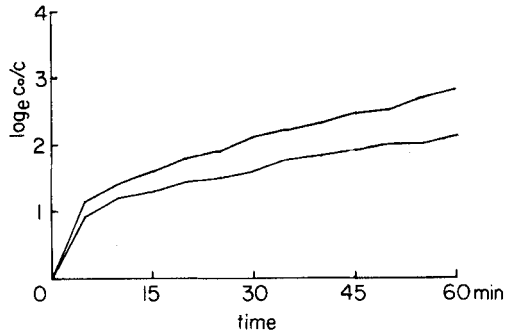

FIG. 6. Methylene blue-TDS; effect of aqueous phase volume. The aqueous phase volume for the upper curve is 200 mL; for the lower, 400 mL. Concentrations: MeBl, 7.10×10^{-6}; NaTDS, 1.4×10^{-5} *M*.

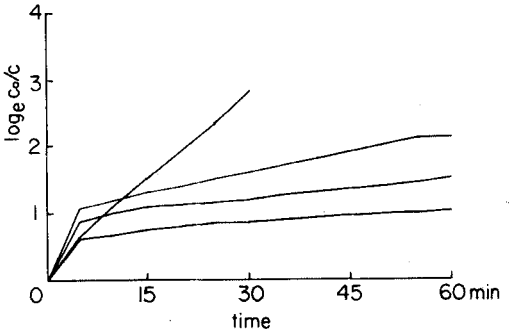

FIG. 7. Methyl orange-HTA; effect of added $NaNO_3$. Concentrations: MeOrange, 5.6×10^{-6}; HTA, 1.1×10^{-5}; $NaNO_3$, 0, 1.9×10^{-4}, 3.7×10^{-4}, and 7.4×10^{-4} *M* (from top to bottom).

octanol. The octanol in the saturated water was sufficient to trap the methylene blue–TDS complex from the aqueous layer during aeration and deposit it on the walls of the column at the top of the aqueous layer. We also noticed that test solutions for spectrophotometric calibration faded slightly over the course of an hour, during which dye accumulated around the walls of the cuvette at the top of the solution.

When runs were made with added salts, persistent foams were observed rising above the octanol layer as much as 10–15 cm before breaking. Negligible quantities of foam were formed during runs made without added salts.

Our work with the methyl orange–HTA system gave much less reproducible results than were obtained with methylene blue–TDS. The effect of

added $NaNO_3$ seemed to be quite a bit larger than was observed with methylene blue–TDS. A run made using tap water (containing considerable calcium) showed almost no removal after the first 5 min of the run. The curvatures of our plots, which exhibit a fast initial removal rate which subsequently decreases markedly, are consistent with Karger's results (*7*). Since these runs were made with water saturated with 2-octanol, we tentatively conclude that the accumulation of octanol in the water layer during the course of a run is not responsible for the curvature. Additional work on this is needed. One standard run and three runs inhibited with varying amounts of $NaNO_3$ are shown in Fig. 7.

THEORETICAL

Removal of Molecular Species

We first examine the situation in which a molecular (nonionic) surface-active, volatile solute is removed from the aqueous phase by solvent sublation. We assume, on the basis of visual observation of our columns in operation, that axial mixing is sufficiently rapid that we may treat the aqueous phase as a single, well-stirred pool. We first examine the rate of change of solute mass associated with a single bubble of (constant) radius as it rises through the water layer. We assume that the rate of mass transfer to the bubble is proportional to the difference between the actual mass of solute associated with the bubble and the mass of solute which would be associated with the bubble (in surface and vapor phases) if the bubble were at equilibrium with the surrounding liquid. This yields

$$\frac{dm_b}{dt} = 4\pi r^2 k \left(\frac{4}{3} \pi r^3 K_w c_w + \frac{4\pi r^2 \Gamma_m}{1 + c_{1/2}/c_w} - m_b \right) \Big/ \frac{4}{3} \pi r^3 \quad (1)$$

where t = time since bubble was formed
m_b = moles of solute associated with bubble
r = bubble radius
k = mass transfer rate coefficient, cm/s
K_w = Henry's law constant for solute in water, = $c_{\text{vapor}}/c_{\text{water}}$ at equilibrium
c_w = solute concentration in aqueous phase, mol/mL
Γ_m = Langmuir isotherm parameter, saturation solute concentration at the air–water interface, mol/cm^2
$c_{1/2}$ = Langmuir isotherm parameter, concentration in the aqueous phase at which the surface concentration is $\frac{1}{2}\Gamma_m$

This equation is easily rearranged to give

$$\frac{dm_b}{dt} + \frac{3}{r}km_b = 4\pi r^2 K\left[K_w c_w + \frac{3\Gamma_m}{r(1 + c_{1/2}/c_w)}\right] \quad (2)$$

Integration of this equation is trivial if one makes the very reasonable approximation that c_w changes negligibly during the time required for the bubble to rise through the aqueous layer. On noting that $m_b(0) = 0$, we obtain

$$m_b(t) = \frac{4\pi r^3}{3}\left[K_w c_w + \frac{3\Gamma_m}{r(1 + c_{1/2}/c_w)}\right]\left[1 - \exp\left(\frac{-3kt}{r}\right)\right] \quad (3)$$

Then the mass of solute carried out of the water layer by one bubble is given by

$$m_b(\text{out}) = \frac{4\pi r^3}{3}\left[K_w c_w + \frac{3\Gamma_m}{r(1 + c_{1/2}/c_w)}\right]\left[1 - \exp\left(\frac{-3kh_w}{ru_w}\right)\right] \quad (4)$$

where h_w = height of water layer

$$u_w = \frac{2g\rho_w r^2}{9\eta_w}\left[1 + \frac{1}{4}\left(\frac{\rho_w r u_w}{2\eta_w}\right) + \frac{0.34\rho_w r u_w}{12\eta_w}\right]^{-1} \quad (5)$$

$= $ bubble rise velocity
g = gravitational constant
ρ_w = aqueous layer density
η_w = aqueous layer viscosity

We next examine the rate of removal of solute from the water layer. We readily find

$$V_w\frac{dc_w}{d\tau} = -N_b\frac{4\pi r^3}{3}\left[1 - \exp\left(\frac{-3kh_w}{ru_w}\right)\right] \times \left[K_w c_w + \frac{3\Gamma_m}{r(1 + c_{1/2}/c_w)}\right] \quad (6)$$

where V_2 = volume of aqueous phase
N_b = number of bubbles introduced into the aqueous phase per second
τ = time from the beginning of the run.

We note that

$$Q_a = 4\pi r^3 N_b/3 \tag{7}$$

where Q_a is the volumetric air flow rate. Separating the variables then yields

$$\frac{dc_w}{K_w c_w + \dfrac{3\Gamma_m}{r(1 + c_{1/2}/c_w)}} = \frac{Q_a}{V_w}\left[1 - \exp\left(\frac{-3kh_w}{ru_w}\right)\right] d\tau \tag{8}$$

This is easily integrated by partial fractions to yield

$$\frac{Q_a}{V_w}\left[1 - \exp\left(\frac{-3kh_w}{ru_w}\right)\right]\tau = \frac{1}{K_w} log_e \frac{c_w(\tau) + c_{1/2} + 3\Gamma_m/K_w r}{c_w(0) + c_{1/2} + 3\Gamma_m/K_w r} + \frac{c_{1/2}}{K_w(c_{1/2} + 3\Gamma_m/K_w r)} \times \log_e \left\{\frac{c_w(\tau)[c_w(0) + c_{1/2} + 3\Gamma_m/K_w r]}{c_w(0)[c_w(\tau) + c_{1/2} + 3\Gamma_m/K_w r]}\right\} \tag{9}$$

from which one can calculate plots of $c_w(\tau)$ as a function of τ for assigned values of the parameters.

This system can also be solved under continuous-flow steady-state conditions. The usual mass balance yields

$$Q_w c_{\text{infl}} = Q_w c_{\text{effl}} + Q_a\left[1 - \exp\left(\frac{-3\text{kh}_\text{w}}{ru_w}\right)\right] \times \left[K_w c_{\text{effl}} + \frac{3\Gamma_m}{r(1 + c_{1/2}/c_{\text{effl}})}\right] \tag{10}$$

One clears this of fractions and solves the resulting quadratic for c_{effl}.

Here c_{infl} = aqueous influent concentration
c_{effl} = aqueous effluent concentration
Q_w = aqueous phase flow rate

In our work with these dye–surfactant species it is certainly safe to assume that the surface-active species is nonvolatile, which permits us to write Eq. (6) as

$$dc_w/d\tau = -A/(1 + c_{1/2}/c_w) \tag{11}$$

This integrates easily to give

$$c_w(t) - c_w(0) + c_{1/2} \log_e [c_w(t)/c_w(0)] = -At \tag{12}$$

Figure 8 shows plots of $\log_e [c_w(0)/c_w(t)]$ versus $At/c_{1/2} \equiv \tau$ for various values of $c_w(0)/c_{1/2}$. These curves are concave upward, approaching linearity as $c_w(0)/c_{1/2}$ approaches zero. This is in disagreement with our experimental curves, which are concave downward. We therefore conclude that the reaction between methylene blue and tetradecyl sulfate does not proceed to completion to form a surface-active species having a Langmuir-type adsorption isotherm.

Mass Transfer Rates

We next consider the problem of estimating k, the mass transfer rate coefficient. We consider solute diffusion through a boundary layer around the rising bubble, and solve the associated diffusion equation with appropriate boundary conditions. This yields an eigenvalue problem, the lowest eigenvalue of which we take as giving an estimate of the mass transfer rate coefficient. For simplicity we treat the case of a volatile, nonsurface-active solute, then show how this is modified for a nonvolatile, surface-active solute.

At the surface of the bubble the chemical potential of the solute in the bordering solution must be equal to the chemical potential of the solute in the (well-mixed) vapor inside the bubble. Outside the bubble we have

$$\mu_e(r) = \mu_e^0 + kT \log_e c(r) \tag{13}$$

where $\mu_e(r)$ = solute chemical potential at r
r = distance from center of bubble
$c(r)$ = solute concentration in solution at r

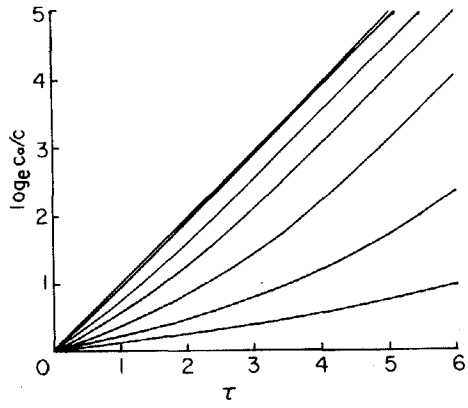

FIG. 8. Removal of molecular species, Langmuir isotherm. Plots of $\log_e C_0/c(t)$ versus $\tau = At/c_{1/2}$ for various values of $c_0/c_{1/2}$. From top to bottom, $c_0/c_{1/2} = 0.125, 0.25, 0.5, 1, 2, 4$, and 8.

Inside the bubble, we have

$$\mu_b = \mu_b^0 + kT \log_e c_b$$

where μ_b = solute chemical potential in the vapor
c_b = solute concentration in the vapor

At the bubble surface these two chemical potentials must be equal, which gives

$$c_b = \lim_{\delta \to 0^+} c(a + \delta) \exp\left[-(\mu_b^0 - \mu_e^0)/kT\right] \tag{14}$$

$$\equiv K_w c(a + \delta), \qquad \delta \to 0^+ \tag{15}$$

where a = bubble radius.

The rate of increase of solute mass in the bubble is given by

$$\frac{dm_b}{dt} = 4\pi a^2 D \frac{\partial c}{\partial r}\bigg|_{r=a} \tag{16}$$

where m_b = moles of solute in bubble $= \frac{4}{3}a^3 c_b$
D = solute diffusion constant in water

So

$$\frac{dc_b}{dt} = \frac{3}{a} D \frac{\partial c}{\partial r}\bigg|_{r=a} \tag{17}$$

Now

$$c_b/K_w = \lim_{\delta \to 0^+} c(a + \delta, t) \tag{18}$$

So

$$\frac{dc_b}{dt} = K_w \frac{\partial c}{\partial t}(a + \delta, t) = \frac{3D}{a} \frac{\partial c}{\partial r}(a, t) \tag{19}$$

from Eqs. (17) and (18). Our boundary condition at $r = a$ is therefore

$$\frac{\partial c}{\partial t}(a, t) = \frac{3D}{aK_w} \frac{\partial c}{\partial r}(a, t) \tag{20}$$

We assume that the boundary layer about the bubble through which diffusion must occur is of thickness $(b - a)$, which gives us a second boundary condition,

$$c(b, t) = c_\infty \tag{21}$$

where c_∞ = solute concentration in the bulk solution.

The differential equation governing diffusion in the boundary layer about the bubble is

$$\frac{\partial c}{\partial t} = \frac{D}{r^2} \frac{\partial}{\partial r}\left(r^2 \frac{\partial c}{\partial r}\right) \tag{22}$$

This is readily solved by separation of variables; we let

$$c = T(t)R(r) \tag{23}$$

to get

$$\frac{\dot{T}}{T} = -\lambda = \frac{D}{r^2 R} \frac{d}{dr}\left(r^2 \frac{dR}{dr}\right) \tag{24}$$

This yields

$$T = \exp(-\lambda t) \tag{25}$$

and

$$\frac{\mathrm{d}}{dr}\left(r^2 \frac{\mathrm{dR}}{dr}\right) + \frac{\lambda}{D} r^2 R = 0 \tag{26}$$

If we let $u/r = R$, we obtain

$$\frac{d^2u}{dr^2} + \frac{\lambda}{D} u = 0 \tag{27}$$

which has as solutions

$$u_0 = A_0 + B_0 r \tag{28}$$

and

$$u_\lambda = A_\lambda \sin \sqrt{\frac{\lambda}{D}}\, r + B_\lambda \cos \sqrt{\frac{\lambda}{D}}\, r \tag{29}$$

Then

$$c(r, t) = \frac{A_0}{r} + B_0 + \frac{1}{r} \sum_\lambda \left[A \sin \sqrt{\frac{\lambda}{D}}\, r + B \cos \sqrt{\frac{\lambda}{D}}\, r \right] e^{\lambda t} \tag{30}$$

As $t \to \infty$ on physical grounds, we must have $c(r, t) \to c_\infty$, $a \leq r \leq b$, which forces us to set A_0 equal to 0 and B_0 equal to c_∞.

The boundary condition at $r = b$, Eq. (21), then yields

$$A_\lambda \sin \sqrt{\frac{\lambda}{D}}\, b + B_\lambda \cos \sqrt{\frac{\lambda}{D}}\, b = 0 \tag{31}$$

On substituting Eq. (30) into Eq. (20) we get, after rearrangement,

$$A_\lambda \left[\sin \sqrt{\frac{\lambda}{D}}\, a \left(\lambda - \frac{3D}{a^2 K_w} \right) + \frac{3D \sqrt{\frac{\lambda}{D}}}{aK_w} \cos \sqrt{\frac{\lambda}{D}}\, a \right]$$

$$+ B_\lambda \left[\cos \sqrt{\frac{\lambda}{D}}\, a \left(\lambda - \frac{3D}{a^2 K_w} \right) - \frac{3D \sqrt{\frac{\lambda}{D}}}{aK_w} \sin \sqrt{\frac{\lambda}{D}}\, a \right] = 0 \tag{32}$$

as our boundary condition at $r = a$. Equations (31) and (32), linear, homogeneous equations, must have nonzero solutions for A_λ and/or B_λ, so the determinant of the coefficients must vanish. This yields

$$0 = \begin{vmatrix} \sin \sqrt{\frac{\lambda}{D}}\, a \left(\lambda + \frac{3D}{a^2 K_w} \right) + \frac{3\sqrt{D\lambda}}{aK_w} \cos \sqrt{\frac{\lambda}{D}}\, a & \sin \sqrt{\frac{\lambda}{D}}\, b \\ \cos \sqrt{\frac{\lambda}{D}}\, a \left(\lambda \quad \frac{3D}{a^2 K_w} \right) - \frac{3\sqrt{D\lambda}}{aK_w} \sin \sqrt{\frac{\lambda}{D}}\, a & \cos \sqrt{\frac{\lambda}{D}}\, b \end{vmatrix} \tag{33}$$

Expansion of the determinant gives

$$\begin{aligned} 0 = {} & \left(\lambda - \frac{3D}{a^2 K_w} \right) \left(\sin \sqrt{\frac{\lambda}{D}}\, a \cos \sqrt{\frac{\lambda}{D}}\, b \right. \\ & \left. - \sin \sqrt{\frac{\lambda}{D}}\, b \cos \sqrt{\frac{\lambda}{D}}\, a \right) + \frac{3\sqrt{D\lambda}}{aK_w} \\ & \times \left(\cos \sqrt{\frac{\lambda}{D}}\, a \cos \sqrt{\frac{\lambda}{D}}\, b + \sin \sqrt{\frac{\lambda}{D}}\, a \sin \sqrt{\frac{\lambda}{D}}\, a \right) \end{aligned} \tag{34}$$

Use of trig identities and rearrangement yields

$$\tan \left[\sqrt{\frac{\lambda}{D}} (b - a) \right] = \frac{3\sqrt{D\lambda}}{aK_w (\lambda - 3D/a^2 K_w)} \tag{35}$$

The smallest positive root of this equation, λ_1, then gives us an estimate of the time constant associated with this diffusion process. For known values of the parameters, Eq. (35) can be solved graphically or numerically for λ_1.

We next need to relate λ_1 to our mass transfer rate constant k; to do this we set $\Gamma_m = 0$ in Eq. (1) (to fit it to the case considered here) and replace m_b by $c_b 4\pi a^3/3$ to get

$$\frac{dc_b}{dt} = \frac{3k}{r}(K_w c_w - c_b) \tag{36}$$

To the limit of our approximation of keeping only one time constant, λ, in our solution, we get from Eqs. (18) and (30) and the initial condition $c_b(0) = 0$, the result that

$$c_b(t) = c_b(\infty)(1 - e^{-\lambda_1 t}) \tag{37}$$

Differentiating Eq. (37) with respect to t yields

$$\frac{dc_b}{dt} = c_b(\infty)\lambda_1 e^{-\lambda_1 t} \tag{38}$$

$$= (-1 + e^{-\lambda_1 t})\lambda_1 c_b(\infty) + \lambda_1 c_b(\infty) \tag{39}$$

$$= \lambda_1 c_b(\infty) - \lambda_1 c_b(t) \tag{40}$$

Comparing this result with Eq. (36) and equating coefficients of $c_b(t)$ then yields

$$k = a\lambda_1/3 \tag{41}$$

as the correspondence between the smallest nonzero eigenvalue of our diffusion problem and the mass transfer rate coefficient for the case of a volatile, nonsurface-active solute.

Ion Pair Equilibrium

We next examine a mechanism for the solvent sublation of ion pairs such as one might expect with hexadecyltrimethylammonium–methyl orange or tetradecyl sulfate–methylene blue. We illustrate the analysis with the system sodium tetradecyl sulfate, methylene blue chloride,

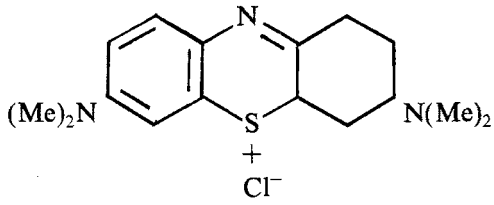

and sodium chloride in aqueous solution. Let

A = tetradecyl sulfate anion
B = chloride
– methylene blue cation
D = sodium ion

In the solution the following ion pair equilibrium takes place

$$AC + BD \rightleftharpoons AD + BC$$

AC, the dye–surfactant complex, and AD, sodium tetradecyl sulfate, are surface active. The equilibrium expression for the above reaction is

$$K_e = \frac{AD \cdot BC}{AC \cdot BD} \tag{42}$$

We assume that the surface concentrations of the surface-active species are given by linear isotherms,

$$\Gamma_{AC} = K_{AC}AC \tag{43}$$

$$\Gamma_{AD} = K_{AD}AD \tag{44}$$

Both AC and BC can be easily detected spectrophotometrically.

There is no mechanism for the removal of chloride by sublation, so we have

$$BC + BD = B_0, \qquad \text{a constant} \tag{45}$$

There is only one way in which methylene blue cation can be removed, so

$$\frac{d}{dt}(AC + BC) = -k_{AC}AC \tag{46}$$

where

$$k_{AC} = \frac{Q_a}{V_w} \frac{3}{r} K_{AC} \left[1 - \exp\left(\frac{-k_{AC} h_w}{r u_w} \right) \right] \tag{47}$$

where k_{AC} = mass transfer rate parameter for AC
r = bubble radius
Q_a = air flow rate
V_w = volume of aqueous phase
h_w = height of aqueous phase
u_w = bubble rise velocity

There are two ways in which tetradecyl sulfate can be removed, so

$$\frac{d}{dt}(AC + AD) = -k_{AC}AC - k_{AD}AD \tag{48}$$

where k_{AD} is defined similarly to k_{AC}.

We now have four equations [(42), (45), (46), and (48)] for the four unknown concentrations AC, AD, BC, BD. Two of these are algebraic, and two are first-order differential equations. It is convenient to change dependent variables to the following set:

$$w = AC + BC \tag{49}$$

$$x = AC + AD \tag{50}$$

$$y = AC - BC \tag{51}$$

$$z = BD \tag{52}$$

The inverse transformation is

$$AC = \tfrac{1}{2}w + \tfrac{1}{2}y \tag{53}$$

$$AD = -\tfrac{1}{2}w + x - \tfrac{1}{2}y \tag{54}$$

$$BC = \tfrac{1}{2}w - \tfrac{1}{2}y \tag{55}$$

$$BD = z \tag{56}$$

Our four equations then become

$$dw/dt = -k_{AC}(\tfrac{1}{2}w + \tfrac{1}{2}y) \tag{57}$$

$$dx/dt = \tfrac{1}{2}(k_{AD} - k_{AC})w - k_{AD}x + \tfrac{1}{2}(k_{AD} - k_{AC})y \tag{58}$$

$$z = B_0 - \tfrac{1}{2}(w - y) \tag{59}$$

$$2K_e = \frac{(-w + 2x - y)(w - y)}{(w + y)z} \tag{60}$$

We use Eq. (59) to eliminate z from Eq. (60), then clear of fractions to get a quadratic equation in y,

$$0 = (K_e - 1)y^2 + (2B_0K_e + 2x)y + (2B_0K_ew - K_ew^2 - 2xw + w^2) \tag{61}$$

In solving the quadratic, we must select that root satisfying the following requirements:

$$y \leq w \qquad \text{(since BC must be} \geq 0)$$

$$y \leq -w + 2x \qquad \text{(since AD must be} \geq 0)$$

$$y \geq w - 2B_0 \qquad \text{(since BD must be} \geq 0)$$

Initial conditions for the numerical integration of Eqs. (57) and (58) are obtained from stoichiometry and equilibrium requirements; initially the nominal concentrations of methylene blue chloride, sodium tetradecyl sulfate, and sodium chloride are BC_0, AD_0, and BD_0, respectively; the initial equilibrium then gives

$$K_e = \frac{(AD_0 - AC)(BC_0 - AC)}{AC(BD_0 + AC)} \tag{62}$$

which yields

$$0 = (1 - K_e)AC^2 - (AD_0 + BC_0 + K_eBD_0)AC + AD_0 \cdot BC_0 \tag{63}$$

We choose the root of this equation satisfying the requirements $AC \geq 0$, $AD = AD_0 - AC \geq 0$, $BC = BC_0 - AC \geq 0$. Also, $BD = BD_0 + AC$.

From these initial concentrations we calculate initial values of w, x, y, and z. Equations (57) and (58) are then integrated forward in time one time increment Δt by means of a standard predictor-corrector method, the new values of w and x are used to calculate y from Eq. (61) and z from Eq. (59), and the process is then repeated for as many time increments as desired. The most readily observable quantity experimentally is w, the sum of the two forms of methylene blue, which is measured spectrophotometrically.

The transcription of the notation to the hexadecyltrimethylammonium cation–methyl orange anion system is straightforward.

Let us next look at some calculated results obtained from this model. Calculations were done on a DEC 1099 computer, and a typical run took only a few seconds of machine time. The plots shown are all plots of $\log_e$[initial total methylene blue/total methylene blue at time t] versus time. This type of plot shows up departures from first-order kinetics particularly clearly.

The effect of varying the equilibrium constant in the ion pair reaction is shown in Fig. 9. Increasing the equilibrium constant shifts the equilibrium away from dye–surfactant pairs. We see the expected decrease in dye removal rate as this occurs, and we also see that these curves are not linear (first-order kinetics), but concave downward. Qualitatively this is in agreement with our experimental results, which show the same behavior.

The effects of decreasing the rate constant for the removal of sodium tetradecyl sulfate are to increase the rate of dye removal and to increase the linearity of the curves, as shown in Fig. 10. If tetradecyl sulfate is removed

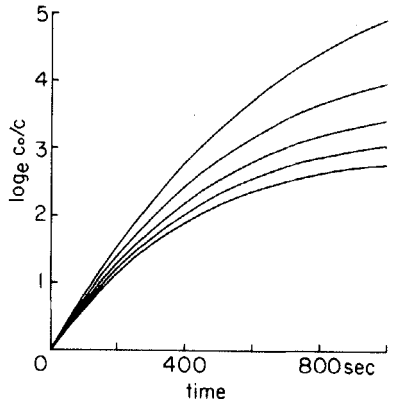

FIG. 9. Removal of ion pairs, linear isotherms. Plots of $\log_e c_0/c(t)$ versus t for various values of K_e. $BD_0 = 0$, $BC_0 = 10^{-3}$, $AD_0 = 2.1 \times 10^{-3}$ mol/L; $k_{AC} = 0^{-2}$, $k_{AD} = 5 \times 10^{-3}$ s^{-1}; $K_e =$ 0.1, 0.2, 0.3, 0.4, and 0.5. from top to bottom. c = total dye concentration.

more slowly as the sodium salt, at any time there will be more of it present in the solution to form floatable ion pairs with the methylene blue, thereby enhancing the rate of removal of the dye.

Decreasing the initial concentration of surfactant decreases the rate and ultimate extent of removal of the dye, as seen in Fig. 11. The plateaus in the curves for runs with relatively small ratios (1:1 or less) of surfactant to dye occur when the surfactant has been essentially completely removed from the solution.

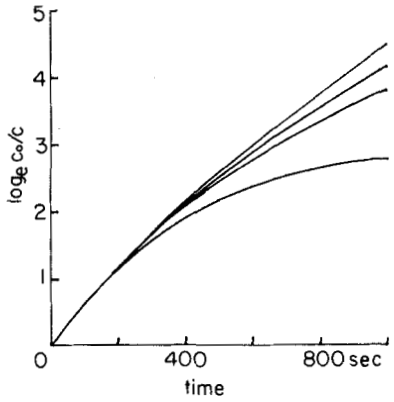

FIG. 10. Removal of ion pairs, linear isotherms. Plots of $\log_e c_0/c(t)$ versus t for various values of k_{AD}. $BD_0 = 0$, $BC_0 = 10^{-3}$, $AD_0 = 2.1 \times 10^{-3}$ mol/L; $K_e = 0.5$; $k_{AC} = 10^{-2}$, $k_{AD} = 0$, 10^{-3}, 2×10^{-3}, and 5×10^{-3} s^{-1} from top to bottom.

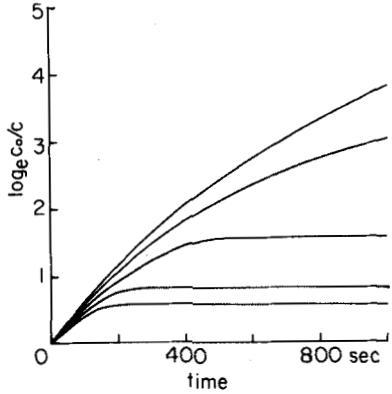

FIG. 11. Removal of ion pairs, linear isotherms. Plots of $\log_e c_0/c(t)$ versus t for various values of AD_0. $BD_0 = 0$, $BC_0 = 10^{-3}$, $AD_0 = 5$, 6.67, 10, 15, and 21×10^{-4} mol/L (bottom to top); $K_e = 0.5$; $k_{AC} = 10^{-2}$, $k = 2 \times 10^{-3}$ s^{-1}.

Within the framework of this mechanism the effect of added salt on the rate of removal of dye can be very great, as seen in Fig. 12. Added salt simply drives the ion pair equilibrium away from dye–surfactant complexes, as expected qualitatively on the basis of a Le Chatelier's principle. This effect is in fact observed with both our dye–surfactant systems, as we've seen in the Experimental Section of this paper. It is not predicted by the mechanism proposed for these processes by Karger et al. (*7*), and it therefore raises some question about the applicability of that mechanism of these ion pair systems. The effect poses a potentially serious problem for those interested in the stripping of such systems from wastewaters or process streams. On the other hand, it provides another possible tool by means of which solvent sublation separations could be made more discriminating and selective.

We note that these curves are concave downward, in agreement with the experimental results, that the inhibiting effect of added salt predicted by the mechanism is observed experimentally, and that the enhancing effect of excess surfactant predicted by the mechanism is also observed experimentally. We also observe, however, that the initial very rapid rise of the experimental plots followed by a slower rise at later times is quite a bit more abrupt than predicted by this model. In fact, we were unable to find parameters to use in the model which yielded curves of that type, and must therefore conclude that this mechanism, attractive though it is, does not adequately describe the flotation of methylene blue with tetradecyl sulfate.

A Second Ionic Equilibrium

Let us consider the reaction

$$\underset{A}{MeBlCl} + 2\underset{B}{NaTDS} \rightleftharpoons \underset{C}{NaMeBl(TDS)_2} + \underset{D}{NaCl}$$

in which a methylene blue ion is bound to two tetradecyl sulfate ions. The equilibrium expression for this reaction is

$$K_e = \frac{CD}{AB^2} = \frac{C(D_0 + C)}{(A_0 - C)(B_0 - 2C)} \tag{64}$$

initially. Here

A_0 = nominal concentration of methylene blue chloride
B_0 = nominal concentration of sodium tetradecyl sulfate
D_0 = nominal concentration of NaCl ($C_0 = 0$).

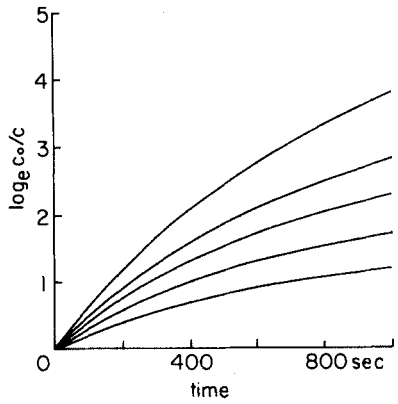

FIG. 12. Removal of ion pairs, linear isotherms. Plots of $\log_e c_0/c(t)$ versus t for various values of BD_0 (added salt). $BD_0 = 0$, 1, 2, 4, and 8×10^{-3} (top to bottom), $BC_0 = 10^{-3}$, $AD_0 = 2.1 \times 10^{-3}$ mol/L; $K_e = 0.5$; $k_{AC} = 10^{-2}$, $k_{AD} = 2 \times 10^{-3}$ s^{-1}.

We solve Eq. (64) to obtain the initial equilibrium concentrations in the system.

Again we assume that the two surface-active species (B and C) are governed by a linear adsorption isotherm. The rate of removal of total methylene blue is then given by

$$\frac{d}{dt}(A + C) = -k_C C \tag{65}$$

The rate of removal of total surfactant is given by

$$\frac{d}{dt}(B + 2C) = -k_B B - 2k_C C \tag{66}$$

There is no way by which Cl^- is removed, which gives

$$A + D = A_0 + D_0 \equiv \alpha_0 \tag{67}$$

As before, we define a new set of dependent variables,

$$w = A + C \tag{68}$$

$$x = B + 2C \tag{69}$$

$$y = \mathrm{A} - \mathrm{C} \tag{70}$$

$$z = \mathrm{D} \tag{71}$$

The inverse transformation is

$$\mathrm{A} = \tfrac{1}{2}w + \tfrac{1}{2}y \tag{72}$$

$$\mathrm{B} = x - 2 + y \tag{73}$$

$$\mathrm{C} = \tfrac{1}{2}w - \tfrac{1}{2}y \tag{74}$$

$$\mathrm{D} = z \tag{75}$$

Equation (67) then becomes

$$\alpha_0 = z + \tfrac{1}{2}w + \tfrac{1}{2}y \tag{76}$$

The equilibrium expression, Eq. (64), becomes

$$K_e = \frac{(\frac{1}{2}w - \frac{1}{2}y)z}{(\frac{1}{2}w + \frac{1}{2}y)(x - w + y)^2} \tag{77}$$

The two rate equations (65) and (66) become

$$dw/dt = -\tfrac{1}{2}k_{\mathrm{C}}w + \tfrac{1}{2}k_{\mathrm{C}}y \tag{78}$$

and

$$dx/dt = (k_{\mathrm{B}} - k_{\mathrm{C}})w - k_{\mathrm{B}}y + (k_{\mathrm{C}} - k_{\mathrm{B}})y \tag{79}$$

Substitution of Eq. (76) for z in Eq. (77) gives

$$K_e = \frac{(w - y)(\alpha_0 - \frac{1}{2}w - \frac{1}{2}y)}{(w + y)(x - w + y)^2} \tag{80}$$

Equations (78), (79), and (80) give us three equations in three unknowns. As before, we integrate Eqs. (78) and (79) forward in time, and calculate y at each time increment by solving Eq. (80) with the new values of w and x. This is readily done by computer; the cubic equation was solved iteratively.

The results were in substantially better agreement with our experimental

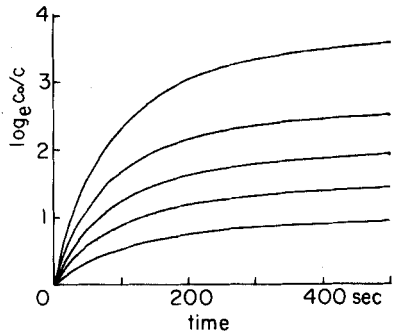

FIG. 13. Removal of 1:2 dye–surfactant complexes, linear isotherms. Plots of $\log_e c_0/c(t)$ versus t for various concentrations of added salt, D_0. $A_0 = 10^{-3}$, $B_0 = 2.1 \times 10^{-3}$, $D_0 = 0, 3 \times 10^{-3}$, 10^{-2}, 3×10^{-2}, and 10^{-1} mol/L (top to bottom); $K_e = 10^4$ L/mol; $k_B = 2 \times 10^{-3}$, $k_C = 4 \times 10^{-2}$ s^{-1}.

data. The inhibition effect of added salt is shown in Fig. 13, and is consistent with our experimental results. The addition of excess surfactant greatly enhances the rate of removal of dye, especially after the separation has been run for some time, as shown in Fig. 14 and consistent with our experimental findings. The curves all are concave downward, in agreement with the

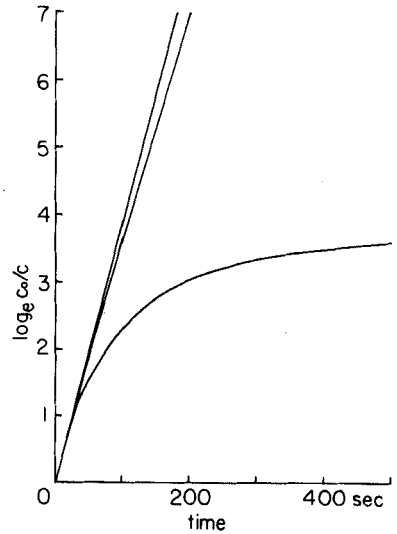

FIG. 14. Removal of 1:2 complexes. Plots of $\log_e c_0/c(t)$ versus t for various values of B_0 (surfactant). $A_0 = 10^{-3}$, $B_0 = 3$, 2, and 1×10^{-3} (top to bottom);, $D_0 = 0$ mol/L, $K_e = 10^4$ L/mol; $k_B = 2 \times 10^{-3}$, $k_C = 4 \times 10^{-2}$ s^{-1}.

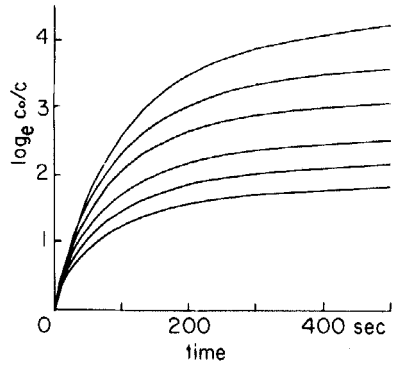

FIG. 15. Removal of 1:2 complexes. Plots of $\log_e c_0/c(t)$ versus t for various values of K_e. $A_0 = 10^{-3}$, $B_0 = 2.1 \times 10^{-3}$, $D_0 = 0$ mol/L; $K_e = 200$, 100, 50, 20, 10, and 5×10^2 L/mol (top to bottom); $k_B = 2 \times 10^{-3}$, $k_C = 4 \times 10^{-2}$ s^{-1}.

experimental data, and they show a very rapid initial rise followed by a substantially flatter portion, also in agreement with the experimental data.

Figure 15 shows the expected enhancement of dye removal with increasing equilibrium constant. From Fig. 16 we see that increasing the rate constant for the removal of NaTDS does not affect the initial rate of dye removal, but decreases the total amount of dye which can be removed. Increasing the rate constant for the removal of dye–surfactant complex, on the other hand, increases both the initial rate of dye removal and the total amount of dye which can be removed, as seen in Fig. 17.

This mechanism, which assumes that (a) a dye–surfactant complex is

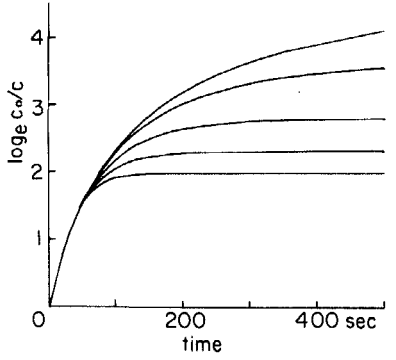

FIG. 16. Removal of 1:2 complexes. Plots of $\log_e c_0/c(t)$ versus t for various values of k_C. $A_0 = 10^{-3}$, $B_0 = 2.1 \times 10^{-3}$, $D_0 = 0$ mol/L; $K_e = 10^4$ L/mol; $k_B = 2 \times 10^{-3}$, $k_C = 2$, 3, 4, 5, and 6×10^{-2} s^{-1} (bottom to top).

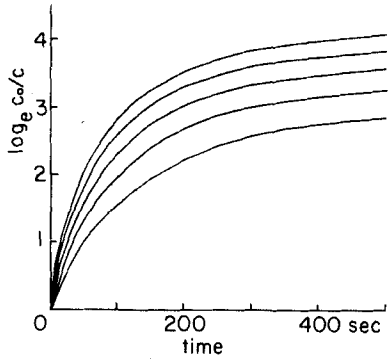

FIG. 17. Removal of 1:2 complexes. Plots of $\log_e c_0/c(t)$ versus t for various values of k_B. $A_0 = 10^{-3}$, $B_0 = 2.1 \times 10^{-3}$, $D_0 = 0$ mol/L; $K_e = 10^4$ l/mol; $k_B = 1, 2, 5, 10$, and 20×10^{-3} (top to bottom), $k_C = 4 \times 10^{-2}$ s^{-1}.

formed which contains 2 mol of surfactant per mole of dye, and (b) this process is a mobile equilibrium, accounts for a number of the features of our experimental plots. The inhibiting effect of added salt, the enhancing effect of excess surfactant, and the peculiar curvature of the plots (concave downward with a rather marked break) observed experimentally are also reflected by the theoretical curves. The other two mechanisms examined produce plots which are qualitatively not in agreement with the experimental results.

These dye–surfactant complexes are convenient to work with because of the ease of doing the analyses, and therefore make useful systems for the development of theory. They are, however, of little significance in terms of waste treatment. We are currently investigating the removal of polychlorinated biphenyls and of some chlorinated hydrocarbon pesticides; preliminary results in lab-scale apparatus look quite promising.

Acknowledgments

This work was supported by a grant from the Office of Water Research and Technology (experimental work) and a grant from the National Science Foundation (theoretical work).

REFERENCES

1. T. Lionel, D. J. Wilson, and D. E. Pearson, *Sep. Sci. Technol., 16,* 907 (1981).
2. F. Sebba, *Ion Flotation*, Elsevier, New York, 1962.
3. B. L. Karger, in *Adsorptive Bubble Separation Techniques* (R. Lemlich, ed.), Academic, New York, 1972, Chap. 8.
4. A. N. Clarke and D. J. Wilson, *Sep. Purif. Methods, 7,* 55 (1978).

5. A. B. Caragay and B. L. Karger, *Anal. Chem., 38,* 652 (1966).
6. B. L. Karger, A. B. Caragay, and S. B. Lee, *Sep. Sci., 2,* 39 (1967).
7. B. L. Karger, T. A. Pinfold, and S. E. Palmer, *Ibid, 5,* 603 (1970).
8. I. Sheiham and T. A. Pinfold, *Ibid., 7,* 43 (1972).
9. M. Bittner, J. Mikulski, and Z. Szeglowski, *Nukleonika, 12,* 599 (1967).
10. J. Elhanan and B. L. Karger, *Anal. Chem., 41,* 671 (1969).
11. P. E. Spargo and T. A. Pinfold, *Sep. Sci., 5,* 619 (1970).
12. Z. Szeglowski, M. Bittner-Jankowska, and J. Mikulski, *Nukleonika, 18,* 299 (1973).
13. Z. Szeglowski, M. Bittner-Jankowska, J. Mikulski, and T. Machej, *Ibid., 18,* 307 (1979).
14. K. Kotsuji, Y. Yameyama, M. Arikawa, and S. Hayashi, *Bunseki Kagaku, 26,* 475 (1977).
15. J. Stachurski, *Chem. Abstr., 81,* 94338 (1974).
16. J. Stachurski and Z. Szeglowski, *Sep. Sci., 9,* 313 (1974).
17. R. B. Grieves, W. Charewiez, and S. M. Brien, *Anal. Chim. Acta, 73,* 293 (1974).
18. A. N. Clarke and D. J. Wilson, *Sep. Sci., 10,* 417 (1975).

Received by editor September 14, 1981